



OPEN

SUBJECT AREAS:

ANATOMY

BIOLOGICAL TECHNIQUES

Received

8 January 2014

Accepted

23 May 2014

Published

12 June 2014

Correspondence and requests for materials should be addressed to Q.Y.G. (gaoqy@mail.sysu.edu.cn)

Preliminary Study on Retinal Vascular and Oxygen-related Changes after Long-term Silicone Oil and Foldable Capsular Vitreous Body Tamponade

Wei Yang, Yongguang Yuan, Yao Zong, Zhen Huang, Shuyi Mai, Yujie Li, Xiaobing Qian, Yaqin Liu & Qianying Gao

State Key Laboratory of Ophthalmology, Zhongshan Ophthalmic Center, Sun Yat-sen University, Guangzhou 510060, China.

Silicone oil has been the only long-term vitreous substitute used in the treatment of retinal detachment since 1962 by Cibis. Nevertheless, its effects on retinal vascular morphology and oxygen supply to the retina are ambiguous in current research. We previously invented a foldable capsular vitreous body (FCVB) to use as a new vitreous substitute in the treatment of severe retinal detachment, but its effects on the retinal vessel were unknown. Therefore, in this study, a standard three-port pars plana vitrectomy (PPV) was performed on the right eye of each rabbit and then silicone oil and FCVB were injected into the vitreous cavity as vitreous substitutes. After 180 days of retention, the retinal vascular morphology did not display any distinct abnormalities, and hypoxia-induced factor-1alpha (HIF-1 α) and vascular endothelial growth factor (VEGF) did not vary markedly during the observation period in silicone oil tamponade- and FCVB-implanted eyes. This study may suggest that silicone oil and FCVB tamponade in rabbit eyes did not cause retinal vascular pathologic changes or retinal hypoxia for 180 days.

More than 95% of the natural vitreous body consists of water, collagens, hydrophilic glycosaminoglycans, metabolites and a few cells. The vitreous body has a gelatinous nature due to its long collagen fibrils suspended in a pattern of hyaluronic acid (HA)¹. The presence of both HA and collagen together facilitates the lower viscoelastic properties of the vitreous^{2,3}. Therefore, the natural vitreous body can act as a metabolic buffering station that transfers metabolites and nutrients from the retina to neighboring tissues via diffusion and convection^{4,5}. Oxygen is one of the most important nutrients, especially for the retina. Under normal circumstances, oxygen diffuses from the retina to the vitreous humour and is then transported to the neighboring tissues⁶. Many vitreoretinopathies necessitate vitrectomy surgery and then the utilization of vitreous substitutes to restore the natural vitreous. Meanwhile, intraocular oxygen diffusion and circulation may be altered by the vitreous substitutes to occur more or less.

Currently, silicone oil is the most commonly used long-term vitreous substitutes in clinic tests⁷. It is known that the kinematic viscosity of human natural vitreous gel and silicone oil used in clinical tests is 300–2,000.cSt and 4,000–5,000.cSt, respectively⁸. Thus, the kinematic viscosity of silicone oil is much higher than that of the vitreous gel^{9,10}. When the addition of silicone oil is highly hydrophobic, its oxygen permeation and diffusion are very weak. Furthermore, its low surface and interfacial tension and low specific gravity create a tamponade effect on the superior retina, which is clearly different from that of the natural vitreous body^{7,11}. Silicone oil is usually preserved in the vitreous cavity for three to six months or, at most, two years, owing to its emulsification and retinal toxicity^{12,13}, and its influence on the retinal oxygen microenvironment during this period requires attention.

We previously invented a foldable capsular vitreous body (FCVB) to replace the natural vitreous body in the treatment of severe retinal detachment in both rabbits and humans¹⁴. It was made of silicone rubber and consisted of a thin vitreous-shaped capsule with a tube-valve system. The capsule was fabricated via a computer simulation of the human and rabbit vitreous cavities and the use of a drainage tube connected to a drainage valve. The medium can be injected into the capsule via the tube-valve system to maintain suitable intraocular pressure and support the retina. The FCVB can provide 360-degree arc support for the retina via its analogous solid strength, which thus provides a new mode of treatment for retinal detachment^{15–17}. When the capsular membrane restored the appearance of the natural vitreous, it segregated the medium from the retina so as to prevent the intraocular

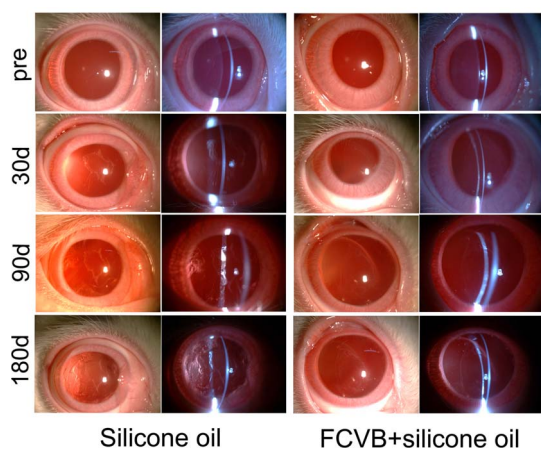


Figure 1 | Preoperative and 30-day, 90-day and 180-day postoperative follow-up examinations using a slit lamp. No severe complications emerged in the anterior segments of the eyes from 30 days to 180 days postoperatively in any of the silicone oil and FCVB + silicone oil groups, except for a slight opacity of the lens posterior capsule in both experimental groups.

toxicity that would be caused by direct contact with the retina and the inordinate flow caused by current vitreous substitutes. In addition, it can avert some severe complications caused by silicone oil emulsification¹⁸. From December 2009 to July 2010, three patients participated in clinical trials (Clinical Trials, gov ID: NCT00910702) and the results demonstrated the preliminary efficacy and safety of the FCVB combined with silicone oil injected in the treatment of severe retinal detachment^{15,19}. From September 2010 to August 2013, we studied 122 participants in multi-center clinical trials at nine ophthalmological hospitals in China successfully (Clinical Trials, gov ID: NCT01261533), and a reliable end result was found in arrangement and statistics analysis. The FCVB acted as a new vitreous substitute and was quoted in the preview of an update on retinal detachment surgery²⁰. Because the FCVB is a new vitreous substitute and utilised a new mode of retina support, which was distinct from those of the natural vitreous body and silicone oil, it is imperative to study its effects on the retina.

At present, many ophthalmopathies, such as diabetic retinopathy and central retinal vein occlusion, can result in evident retinal hypoxia, which can increase hypoxia-related cytokines and then lead to neovascularization generated in the retina and choroid²¹. Up to now,

the most important factors associated with hypoxia have been hypoxia-inducible factor-1alpha (HIF-1 α) and the vascular endothelial growth factor (VEGF)^{22–25}.

Therefore, in this study, we investigate the morphological changes of retinal vessels and the relevant hypoxia cytokines' expression variation in silicone oil tamponade- and FCVBs combined with silicone oil that are implanted into the vitreous cavity of rabbits for 180 days.

Results

Slit lamp. Anterior chamber inflammation was almost visible in both treated groups in the early postoperative period and a few rabbits in the FCVB + silicone oil group had relatively severe cases, with some inflammatory fibrinous exudation in the anterior chamber. However, they recovered within one week postoperatively when given anti-inflammatory treatments. Except for lens posterior capsular opacity, there were no serious complications, such as keratopathy, posterior synechia or iris neovascularization observed over 180 days (Fig. 1).

Because the lens had been removed in the two treated groups, only feeble lens posterior capsular opacity emerged in a few rabbits in each group within 30 days of the operation. Even 180 days after the operation, the opacity of the lens posterior capsule still remained inconspicuous. In the silicone oil group, there was 27.8% opacity (5/18) at 180 days postoperatively and the FCVB + silicone group showed 44.4% opacity (8/18) at 180 days postoperatively.

Intraocular pressure (IOP). The changes in IOPs after surgery are shown in Fig. 2. The IOPs of the silicone oil and FCVB + silicone oil groups maintained relatively gentle fluctuation within the normal range during the postoperative observational period, and regarding the IOPs, no statistically significant differences were found between the two treated groups and contralateral control eyes, either preoperatively or at 7, 14, 30, 60, 90 and 180 days postoperatively ($p > 0.05$). However, a downward trend was evident at day 3 postoperatively in the silicone oil group ($p = 0.001$) and FCVB + silicone group ($p < 0.001$) as compared to the contralateral eyes. This may have been caused by a postoperative inflammation reaction, which led to a decline of aqueous humor creation.

Fundus photographs and fluorescein angiography. Fundus photographs demonstrated that the fundus could clearly be observed, although a mild opacity in the lens posterior capsule existed at the early and later postoperative stage, and no abnormalities, such as choroiditis, retinal hemorrhage, retinal hole or retinal detachment, were discovered in the two treated groups (Fig. 3). Also, the optic

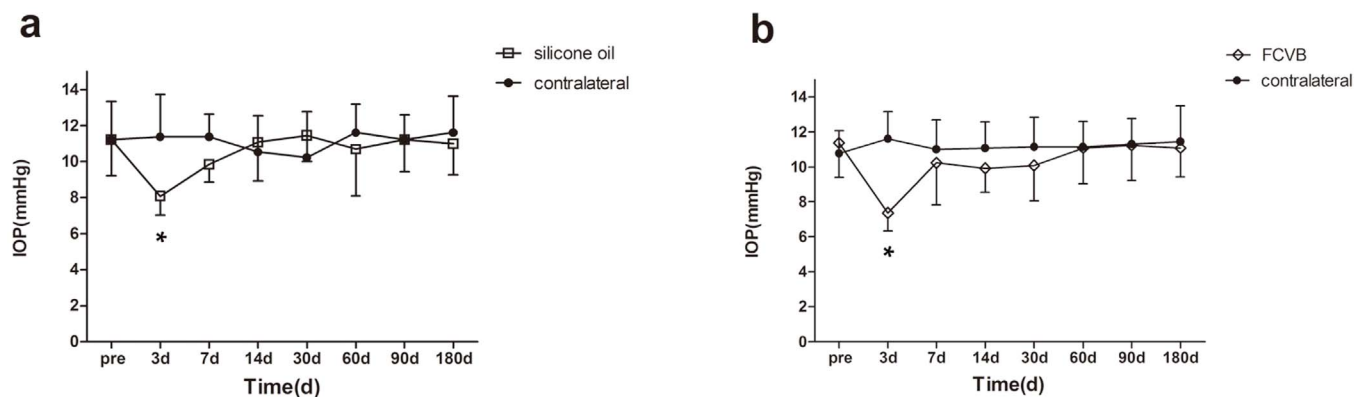


Figure 2 | The fluctuation of intraocular pressure during the 180-day follow-up. No significant differences in intraocular pressure were observed preoperatively or at 7, 14, 30, 60, 90 and 180 days postoperatively among the two treated groups compared to the contralateral eyes ($p = 0.990$, $p = 0.178$, $p = 0.654$, $p = 0.258$, $p = 0.398$, $p = 0.942$ and $p = 0.693$ in the silicone oil group, respectively; $p = 0.682$, $p = 0.578$, $p = 0.354$, $p = 0.258$, $p = 0.898$, $p = 0.942$ and $p = 0.791$ in the FCVB group, respectively). But a significant decrease was observed at day 3 postoperatively in the silicone oil group and FCVB groups compared to the contralateral eyes ($p = 0.001$; $p < 0.001$). Error bars represent the mean squared error (SEM) (* $p < 0.05$).

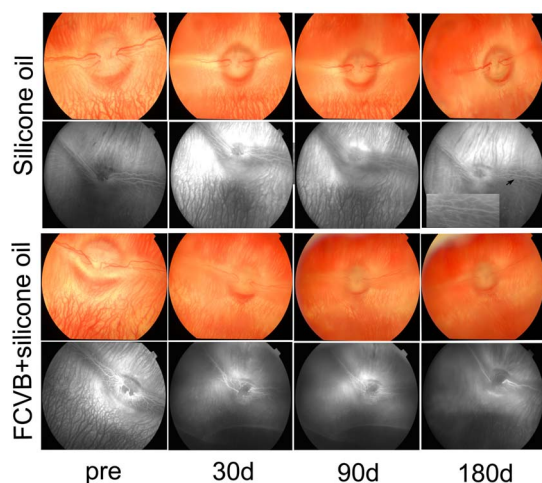


Figure 3 | Preoperative and postoperative fundus photography and fluorescein angiography. The two treated groups had no abnormal events within 180 days. All eyes showed clarity in the vitreous cavities, except that some appeared to be mildly blurry due to lens posterior capsular opacity in both groups. Fluorescent leakage dots were observed in the silicone oil group postoperatively (black arrow).

disk's appearance and boundary was clear, and no tortuosities, vasodilatations or microaneurysms in the medullary wings and/or peripheral capillaries were observed.

Preoperative fundus fluorescein angiography results (Fig. 4) and those at 30, 90 and 180 days postoperatively showed complete consistency with the fundus photographs (Fig. 3). The retinal vessels were unobstructed and no pathological fluorescein leakages, neovascularization, aneurysms or areas of capillary non-perfusion in the periphery of the medullary wing appeared. Similarly, no capillary tortuosity and distinct ischemic regions with vascular shunts were documented in either group, except for some fluorescent dots in the

early stage (Fig. 4, white arrow) to the later preoperative stage (Fig. 4, black arrow), as well as postoperatively (Fig. 3, black arrow), which we did not consider to be a pathologic alteration, as they may have been caused by the specific retinal vascular structure of New Zealand albino rabbits.

Expression of total retinal HIF-1 α and VEGF mRNA. As shown in Fig. 5a, no significant variations were observed in HIF-1 α mRNA at 30, 90 and 180 days postoperatively in the silicone oil and FCVB + silicone oil groups ($p = 0.209$, $p = 0.853$ and $p = 0.797$ in the silicone oil group, respectively; $p = 0.147$, $p = 0.966$ and $p = 0.543$ in the FCVB + silicone oil group, respectively) compared to the contralateral control eyes. As shown in Fig. 5d, similarly, in regard to VEGF mRNA expressions, no statistically significant difference was found between the silicone oil and the FCVB + silicone oil group at 30, 90 and 180 days postoperatively in this regard ($p = 0.685$, $p = 0.350$ and $p = 0.567$ in the silicone oil group, respectively; $p = 0.984$, $p = 0.135$ and $p = 0.516$ in the FCVB + silicone oil group, respectively).

Expression of retinal HIF-1 α protein. As shown in Fig. 5b and c, the results of the HIF-1 α protein Western blot showed no statistically significant differences in the silicone oil and FCVB + silicone oil group compared with the contralateral eye control group at 30, 90 and 180 days postoperatively ($p = 0.163$, $p = 0.684$ and $p = 0.820$ in the silicone oil group, respectively; $p = 0.169$, $p = 0.678$ and $p = 0.719$ in the FCVB + silicone oil group, respectively).

VEGF protein concentrations, as detected by ELISA. The normalized VEGF protein concentrations in the retinas at 30, 90 and 180 days postoperatively are shown in Table 1 and Fig. 5e. No significant differences were noted at 30, 90 and 180 days postoperatively in the silicone oil group ($p = 0.745$, $p = 0.437$ and $p = 0.891$, respectively) or the FCVB + silicone oil group ($p = 0.564$, $p = 0.335$ and $p = 0.744$, respectively) as compared to the contralateral eyes.

Histopathologic findings. There was no evidence of pathological changes in retinal tissues or structural abnormalities, such as

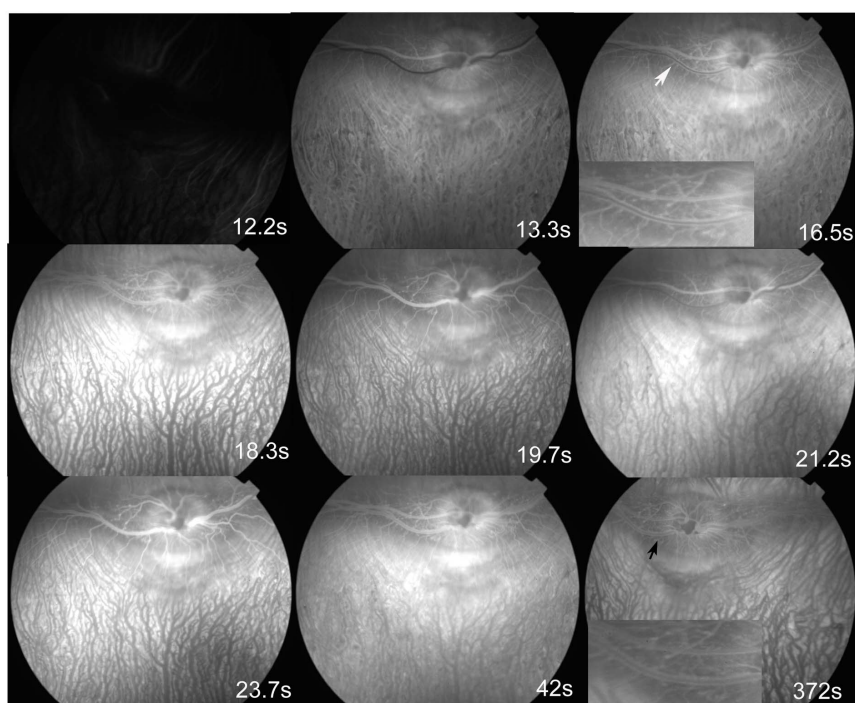


Figure 4 | The main stages of fundus fluorescein angiography in a normal New Zealand albino rabbit preoperatively. The pre-arterial phase (10.2 s), the arterial phase (13.3 s), the arteriovenous phase (16.5 s), the venous phase (19.7 s) and the later period (372 s) are shown. Some fluorescein leakage spots were displayed from the arteriovenous phase (white arrow) to the later phase (black arrow).

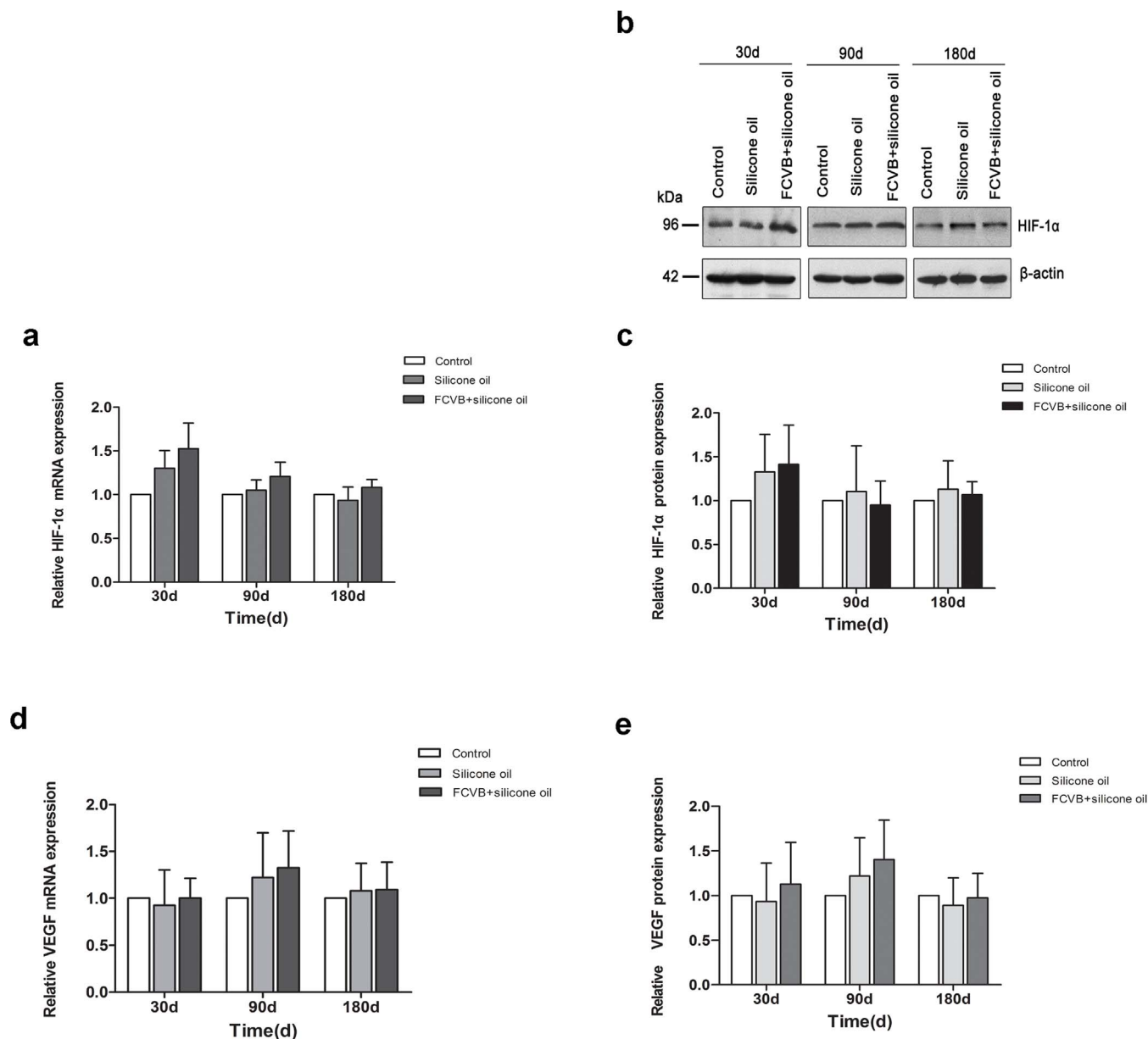


Figure 5 | The relative mRNA and protein expressions of HIF-1 α and VEGF in the retina postoperatively. No significant variations were found between the HIF-1 α mRNA and protein in the silicone oil and FCVB + silicone oil groups at 30, 90 and 180 days postoperatively compared with the contralateral eyes (Fig. 5 a, b, c) (mRNA: $p = 0.209$, $p = 0.853$ and $p = 0.797$ in the silicone oil group, respectively; $p = 0.147$, $p = 0.966$ and $p = 0.543$ in the FCVB + silicone oil group, respectively. Protein: $p = 0.163$, $p = 0.684$ and $p = 0.820$ in the silicone oil group, respectively; $p = 0.169$, $p = 0.678$ and $p = 0.719$ in the FCVB group, respectively), and no significant differences were shown in the VEGF mRNA and protein in both treated groups at 30, 90 and 180 days postoperatively compared with in the contralateral eyes (d, e) (mRNA: $p = 0.685$, $p = 0.350$ and $p = 0.567$ in the silicone oil group, respectively; $p = 0.984$, $p = 0.135$ and $p = 0.516$ in the FCVB + silicone oil group, respectively. Protein: $p = 0.745$, $p = 0.437$ and $p = 0.891$ in the silicone oil group, respectively; $p = 0.564$, $p = 0.335$ and $p = 0.744$ in the FCVB + silicone oil group, respectively). The statistic data of each treated group is the ratio of HIF-1 α or VEGF levels in the right (treated) eye to that in the left (contralateral) eye ($n = 5$ per group). Error bars represent the SEM.

deformations, degeneration or inflammation, in either of the two groups (Fig. 6). Moreover, there were no pathological alterations in other parts of the eye, including the cornea and ciliary body. In general, the retinal architecture remained well preserved in both silicone oil tamponade- and FCVB + silicone oil- implanted eyes.

Immunohistochemical staining analysis. To investigate the spatial and temporal expressions of HIF-1 α and VEGF in the retina, we performed immunohistochemical staining on retinal cross-sections at 90 and 180 days postoperatively. As shown in Fig. 7, we had not observed any evident staining of HIF-1 α in the normal retina in the control eyes. And also, there was no obvious staining of HIF-1 α in the

retina in the silicone oil and FCVB + silicone oil eyes at 90 and 180 postoperative days. The staining for VEGF was faintly though positively in the normal retina in the control eyes. And VEGF was weak though positively stained in the same retinal region as the control eyes in the two treated groups' eyes at 90 and 180 days postoperatively.

Discussion

Our study demonstrated that there were no obviously macroscopic pathological changes in the morphology and anatomical structure of the retinal vessels. At the same time, there was no up-regulation of HIF-1 α and VEGF in both the silicone oil tamponade- and FCVB +



Table 1 | Relative Normalized VEGF Protein Levels in the Retina (ELISA Assay)

Treated group	Time point	Normalized VEGF (pg VEGF/mg protein) OD[*]	Normalized VEGF (pg VEGF/mg protein) OS[**]	Relative normalized VEGF (OD/OS)[***]
Silicone oil	30 d	20.83 ± 2.39	18.07 ± 3.27	0.92 ± 0.11
	90 d	22.78 ± 1.34	19.35 ± 2.21	1.23 ± 0.05
	180 d	27.53 ± 1.73	20.28 ± 3.44	0.88 ± 0.08
FCVB + silicone oil	30 d	13.76 ± 2.91	20.37 ± 2.53	1.15 ± 0.12
	90 d	28.92 ± 2.81	22.35 ± 2.21	1.43 ± 0.07
	180 d	25.63 ± 1.98	29.44 ± 1.32	0.94 ± 0.06

The values were expressed as mean ± standard deviation (n = 5 per group).

*The mean value of each rabbit oculus dexter;

**The mean value of each rabbit oculus sinister;

***The mean ratio value of each rabbit normalized VEGF oculus dexter/normalized VEGF oculus sinister.

silicone oil-implanted eyes for 180 days in rabbits. This study suggested that silicone oil and FCVBs did not gravely impact retinal vascular morphology or the retinal oxygenous microenvironment of intravitreal tamponade for 180 days in rabbits.

No significant changes in IOP were observed after 7, 14, 30, 60, 90 and 180 days, except for a slight decline at day 3 postoperatively in the two treated groups compared to the contralateral eyes, which may have resulted from the aqueous humour secretion decline caused by ciliary body dysfunction after lensectomy and vitrectomy surgeries^{18,26}. Maintaining normal IOP was essential in this study because the IOP directly influenced ocular perfusion pressure, which is closely correlated to blood flow to the retina. Exorbitant IOP would thus reduce retinal blood flow and simultaneously decrease the retinal oxygen supply²⁷.

In our previous study, most of the eyes were prone to developing cataracts after the FCVBs were implanted for a long time^{18,26}. In addition, cataracts were a common complication of long-term silicone oil tamponade. In order to ensure better postoperative fundus observation, we had to perform a lensectomy to avoid secondary cataracts. Hence, phacoemulsification was performed before vitrectomy in the silicone oil tamponade- and FCVB-implanted eyes.

The preoperative fundus fluorescence angiography of normal New Zealand albino rabbits manifested some fluorescence leakage dots from early-stage (Fig. 4, white arrow) to later-stage angiography (Fig. 4, black arrow). Aside from these fluorescence leakage dots, no abnormalities were displayed. We did not consider these fluorescence leakage dots to be pathological fluorescence exudation. Perhaps they were caused by the particular retinal vascular structures of the New Zealand albino rabbit.

The fundus photography and fundus fluorescence angiography revealed no apparent abnormalities in the retinal vascular morphology or the anatomical structure in the silicone oil and FCVB+ silicone oil

group, which indicated that silicone oil and FCVBs did not exert grave influence on the retinal vessels over 180 days. Relevant clinical cases reporting fluorescent angiographic findings in patients of intravitreal silicone oil retention for more than one year revealed that the arterioles appeared to be narrow and occluded, with an extensive capillary non-perfusion area. In addition, mottled microaneurysms were observed throughout the retina²⁸. Our study results were much different than those obtained in this case report. It should be considered that the duration of silicone oil implantation (over one year) in this case report far exceeded 180 days; the fluorescent angiographic changes described above could have been caused by the toxic intraocular effects of silicone oil on the retinal microvasculatures and by secondary damage to the neuroretina²⁹. An alternative explanation for the observed fluorescein findings is that silicone droplets had invaded the retinal arterioles and mechanically obstructed them³⁰. These toxic side effects of silicone oil will become more prominent as time goes on. In our study, the observation period was too short to cause obvious retinal toxic side effects.

Our study results revealed that the expressions of HIF-1 α and VEGF did not up-regulate in the retinas at 30, 90 or 180 days postoperatively in the two experimental groups. HIF acts as a ubiquitously expressed master regulator of oxygen homeostasis³¹. HIF-1, the most important member of the HIF family, is a complex heterodimeric protein consisting of an oxygen-dependent subunit (HIF-1 α) and a constitutively expressed nuclear subunit (HIF-1 β). Under normoxic conditions, HIF-1 α experiences ubiquitylation and proteasomal degradation. Under hypoxic conditions, HIF-1 α is stabilized, binds with HIF-1 β and activates the transcription of various target genes^{32–34}. Nevertheless, VEGF has constitutive, low-level expression in normal ocular tissues, which is consistent with serving as a vascular survival factor^{35–37}. VEGF expression was observed in the inner retina, particularly in the ganglion cells, outer

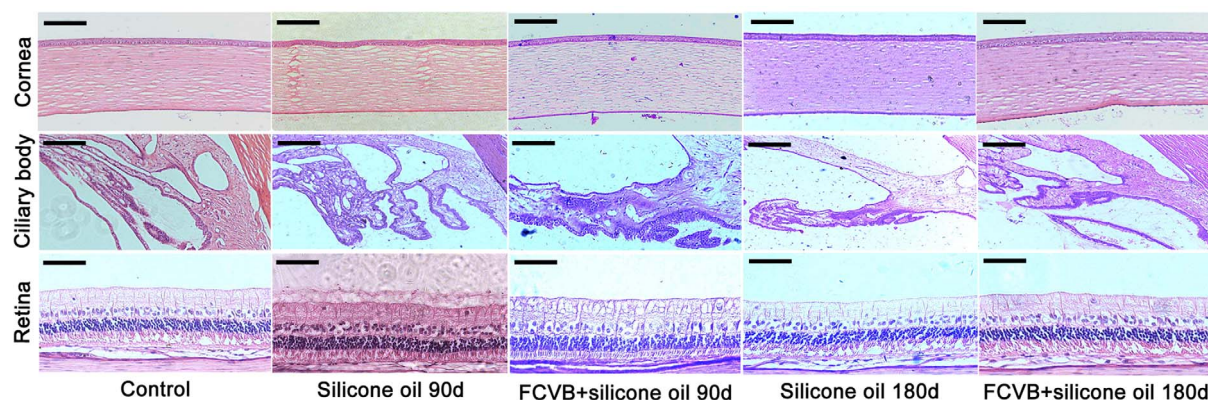


Figure 6 | Histology revealed the normal structure and cell morphology of the eyeball in the two groups after 90 days and 180 days. No evidence of pathological changes or structural abnormalities in the cornea, ciliary body or retina was seen, and no disorganization of the retina was displayed in the two experimental groups. (Scale bars, 50 μ m; n = 4 per group).

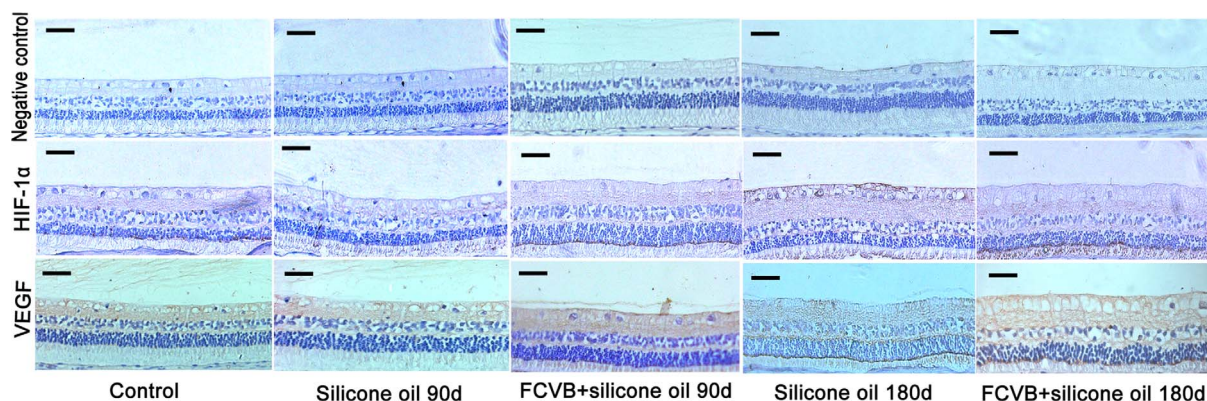


Figure 7 | The spatial and temporal expressions of HIF-1 α and VEGF in the retina. VEGF were faint positively staining in the inner retinal layers of the contralateral eyes. The same faint positively expressions in the inner retinal layers were found in the silicone oil and FCVB + silicone oil groups at 90 days and 180 days postoperatively. No remarkable positive staining of HIF-1 α was demonstrated in the contralateral eyes and the two treated groups' eyes at each time point. (Scale bars, 50 μ m; n = 4 per group).

nuclear layer, visual cortex cell layer and pigment epithelium layer^{37–39}, which was consistent with our study results. Under hypoxic conditions, VEGF expression will markedly increase in these regions of the retina.

HIF-1 α regulates the expression of a variety of oxygen-regulated factors, including VEGF^{40,41}. HIF-1 α plays an important role in the initial increase in VEGF mRNA in response to hypoxia⁴². The sequential occurrence of the onset of hypoxia will increase the levels of HIF-1 α and VEGF expression. Therefore, HIF-1 α and VEGF expressions have a temporal and spatial correlation⁴³; that is, VEGF's expression is delayed behind that of HIF-1 α , and the HIF-1 α and VEGF express in the inner retinal layer, but they are not uniform among all cell types. Of course, oxygen may not be the sole physiological stimulus for VEGF expression's up-regulation in vivo. Hypoglycemia, reactive oxygen intermediates, insulin-like growth factor-1 and advanced glycation end products are known stimuli that exist in the eye and are capable of promoting VEGF expression. They may facilitate the modulation of VEGF expression in eyes^{44,45}.

In our study, the HIF-1 α and VEGF did not elevate in silicone oil tamponade- or FCVB-implanted rabbits' eye, it implied that no retinal hypoxia occurred during the silicone oil and FCVB-intraocular-tamponade period. Retinal oxygen was supplied by the retinal and choroid blood vessel, and was then diffused and convected to the

surrounding intraocular tissues via the vitreous body⁴⁶. A criteria and guideline for ideal biomaterial vitreous substitutes proposed an assessment of the viscoelastic properties and diffusion coefficient of a model solute^{47,48} and the diffusion coefficient is closely related to the kinematic viscosity of the vitreous substitute; the higher its viscoelasticity, the lower the diffusion coefficient it possesses on the basis of the diffusion coefficient formula of gas movement in the liquid phase^{49,50}. Because silicone oil is more viscous than vitreous gel^{8–10}, according to the diffusion coefficient formula, the diffusion and transport of all molecules in silicone oil is slowed accordingly and it reestablishes the diffusion barrier between the retina and vitreous humour^{6,8,51,52}.

However, because the solubility of oxygen in silicone oil is extremely high, and reported to be 20 \times higher than in water by Poncelet⁵³, dissolved oxygen content in silicone oil is much higher than in water, with a related study showing that oxygen content in silicone oil was obviously higher than in the vitreous body after vitrectomy⁵⁴. The high oxygen solubility and poor diffusion of silicone oil are antagonistic in oxygen convection and circulation. It is hard to figure out which plays a predominant role in oxygen circulation and redistribution in intraocular tissues. However, on the basis of our study results, we had reasonable ground to believe the silicone oil was highly oxygenated in the vitreous cavity and could not have a serious impact on the posterior eye segment and the retina's oxygenic environment.

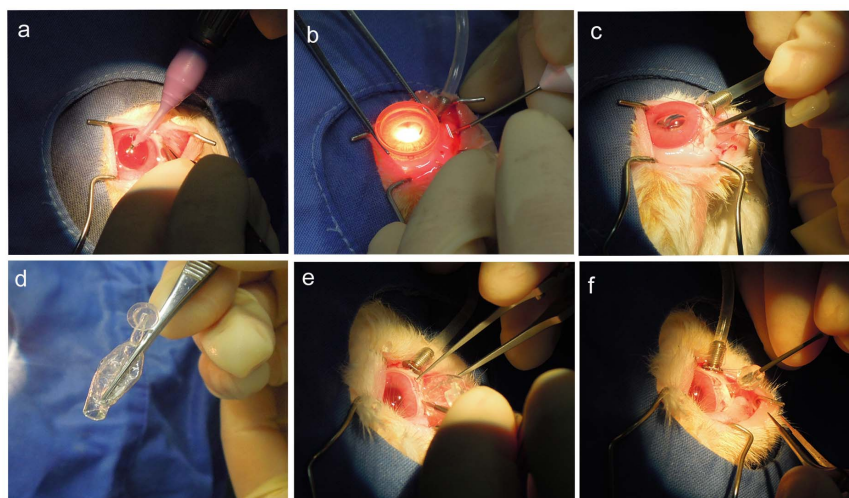


Figure 8 | Rabbit surgical procedures. (a): A standard PHACO was performed to remove the lens. (b): A standard three-port PPV was performed to remove the vitreous. (c): The silicone oil was injected into the vitreous cavity. (d–e): The FCVB was folded and implanted into the vitreous cavity. (f): The silicone oil was injected into the capsule through the valve.



Table 2 | Primers for Real-time PCR Amplification

Cytokine	Accession No. (Life Technologies)	Forward Primer	Reverse Primer
HIF-1 α	A12926	TTACAGCAGCCAGATGATCG	TGGTCAGCTGTGGTAATCCA
VEGF	A12926	CTACCTCCACCATGCCAAGT	AGATGTCCACCAAGGTCTCG
GAPDH	A12926	GGAATCCACTGGCGTCTCA	GGTTCACGCCCATCACAAC

In the FCVB capsule, mini-apertures of 300 nm were detected via the scanning electron microscope^{17,55} and in our previous studies, we noted that these mini-apertures can slowly release micromolecular substances, such as dexamethasone sodium phosphate⁵⁶, 5-fluorouracil (5-Fu)⁵⁷ and siRNA-PKC α ⁵⁵. Therefore, the thin capsule membrane was highly oxygen permeable due to the mini-apertures. In addition, the capsule membrane was very thin (thickness 0.06 ± 0.02 mm)¹⁷. In the meantime, we maintained normal IOPs in FCVB-implanted eyes throughout the 180-day period. From the above, we considered that the possible mechanical pressure of the FCVB capsule membrane to the retina was very weak, so retinal hypoxia did not arise in FCVB-implanted eyes.

In our study, we implanted the silicone oil and FCVB into normal New Zealand albino rabbits' vitreous cavities as experimental models. However, the rabbit retina is semi-vascularized, its retinal vessels start from the optic disk and alary distribute on both sides, the vascular coverage retinal areas are limited, and the supply of oxygen and nutrients of the rest of the retina area depend on the choroid, which obviously differs from that of humans, which may be a flaw of this study.

Silicone oil is typically removed from the vitreous cavity after three to six months due to silicone oil's emulsification complications and toxic retinal effects⁵⁸. It is imperative to prolong the observation time in order to further explore the long-term effects of vitreous substitutes on retinal vascular and retinal hypoxia variation. In addition, although the fundus fluorescence angiography did not display any apparent changes in the retinal vascular morphology and anatomical structures, further studies should be performed on the retinal vascular subcellular structure's alteration via electron microscope. Moreover, haemodynamics and oxyhemoglobin saturation should be evaluated after long-term silicone oil tamponade and FCVB implantation. In the meantime, our group is performing relative research on the retina vascular oxygen saturations of silicone oil tamponade- patients via a non-invasive retinal oximeter (Oxymap T1; Oxymap ehf., Reykjavik, Iceland), which can deepen and improve research on the effect of silicone oil on the retinal oxygenic microenvironment and metabolism in some ways.

In this study, we set three time points (30, 90 and 180 days postoperatively) so as to continuously monitor HIF-1 α 's and VEGF's dynamic variational characteristics during the vitreous substitutes' intravitreal tamponade period. In this way, we found that HIF-1 α and VEGF did not vary significantly during the observation period in silicone oil tamponade- and FCVB-implanted eyes. The unchanged expressions of HIF-1 α and VEGF suggested no emergence of retinal hypoxia. In addition, the fundus fluorescence angiography did not show any macroscopic pathological changes in the retinal vascular morphology and structures. Therefore, this study may provide a theoretical basis for the safe application of the FCVB in clinical settings. Additionally, we can now focus on the vitreous substitutes' effect on the retinal oxygenic microenvironment and provide a reference index for the development of the desired vitreous substitutes.

Methods

The rabbit FCVB. The rabbit FCVB (Guangzhou Vesber Biotechnology Co. Ltd., Guangzhou, China) was made of tailor-made modified liquid silicone rubber. The basic material was Dow Corning Class VI elastomers (Dow Corning Corporation, Midland, MI, U.S.A.) and the shape was fabricated by mimicking the vitreous parameters of the rabbit. The FCVB consisted of a vitreous-shaped capsule, a tube and a valve. The standard weight of the FCVB for rabbits was 0.21 ± 0.005 g and the

standard thickness of the capsular film for rabbits was 0.06 ± 0.02 mm. More fabrication details were found, as previously described¹⁷. The FCVBs were sterilized via autoclaving for 20 minutes before surgery.

Animal surgical procedures. All experiments were performed in accordance with the Association for Research in Vision and Ophthalmology (ARVO) statement regarding the use of animals in ophthalmic and vision research. The study protocol was reviewed and approved by the animal experimental ethics committee of Zhongshan Ophthalmic Center, Sun Yat-sen University, China (authorized number: 2012-004). Forty-six New Zealand albino rabbits weighing 2.5 to 3.0 kg were used in this study. All the rabbits were randomly divided into two groups: The FCVBs were implanted into the vitreous cavities and then injected with silicone oil (FCVB + silicone oil group, $n = 23$), or silicone oil tamponade only (Silicone oil group, $n = 23$).

All surgeries were performed while following aseptic principles. After pupillary dilatation with 1% tropicamide (Mydrin P, Santen, Osaka, Japan), the rabbits were anesthetized via an intramuscular injection of a mixture of ketamine hydrochloride (30 mg/kg) and chlorpromazine hydrochloride (15 mg/kg). Under the standard ophthalmic operating microscope (OPMI VISU 200 plus; Carl Zeiss, Jena, Germany), a standard three-port pars plana vitrectomy (PPV) was performed on the right eye of each rabbit using the 20-gauge Alcon Accurus vitrectomy system (Fig. 8.b). A standard phacoemulsification (PHACO) was performed using the Alcon phaco-emulsification system (LEGACY system Series 20000; Alcon, U.S.A.) to remove the lens prior to PPV (Fig. 8.a). After finishing the phacoemulsification and vitrectomy in the FCVB + silicone oil group, the FCVBs were folded into three petals and implanted into the vitreous cavity by lengthening the original sclera incision at 12 o'clock to 3 mm, without fluid-air exchange (Fig. 8.d, e). Then, 1.2 ml of silicone oil (Acri.Silol 5000; Acri.Tec, GmbH, Berlin, Germany) was injected into the capsule through the tube-valve device (Fig. 8.f) and the valve was subsequently fixed under the conjunctiva. In the silicone oil group, 1.2 ml of silicone oil was injected directly into the vitreous cavity after complete fluid-air exchange (Fig. 8.c). At the same time, the intraocular pressure was carefully adjusted to a normal level (9 to 18 mmHg)⁵⁹ via injected silicone oil. The left eye did not undergo surgery and served as the contralateral control. The surgery ended with a subconjunctival injection of tobramycin and dexamethasone.

After surgery, the eyes were treated with tobramycin dexamethasone eye drops (Tobradex, Alcon, U.S.A.) and pranoprofen eye drops (Pranopulin, Senju, Japan) three times a day for two weeks.

Postoperative examinations. After surgery, a slit lamp (SL-D7; Topcon Co., Japan) and a fundus camera (TRC-50DX; Topcon Co., Japan) were used to examine and record the anterior segment, ocular media and fundus preoperatively and at days 3, 7, 14, 30, 60, 90 and 180 postoperatively. A Tono-Pen (Tonopen AVIA; Reichert Co., U.S.A.) was used to measure intraocular pressure (IOP) preoperatively and at day 3, 7, 14, 30, 60, 90 and 180 postoperatively.

Fundus fluorescein angiography. Fundus fluorescein angiography was performed preoperatively and at days 30, 90 and 180 postoperatively. This operation was performed under general anesthesia and pupil dilation. After fixing the appropriate location of the rabbit and aiming at the fundus, an intravenous injection of sodium fluorescein (10%, 0.1 ml; Alcon, U.S.A.) via the marginal ear vein was performed. The fundus images and angiograms were immediately obtained via the fundus camera (TRC-50DX; Topcon Co., Japan) from 1 second to 15 minutes.

Isolation of total RNA. In each group, five rabbits were executed by overdose injection of ketamine and chlorpromazine (1 : 1) on days 30, 90 and 180 postoperatively. Then, both eyes were harvested from these rabbits and the retinas were isolated under an ophthalmic anatomic microscope (SteREO Discovery V.8; Carl Zeiss, Germany). The total RNA was extracted from the retinas with TRIzol Reagent (Invitrogen Trizol, CA, U.S.A.) and 200 ml/L of chloroform was added to the retina homogenates with Trizol. This mixture was then shaken vigorously for 15 seconds, kept at room temperature for 5 minutes and centrifuged at 12,000 rpm for 15 minutes at 4°C ultracentrifuge (Eppendorf 5415R; Eppendorf AG, Germany). The supernatants were collected. One ml of isopropanol was added. These were mixed, kept at room temperature for 5 minutes and then centrifuged at 12,000 rpm for 15 minutes at 4°C. The aqueous phases were removed and the RNA precipitates were washed with 75% ethanol, centrifuged at 8,000 rpm at 4°C for 5 minutes, air dried and solubilized in diethylpyrocarbonate (DEPC)-treated water (R0021; Beyotime, Beijing, China). The purity and concentrations of the RNA were assessed via a spectrophotometric measurement (Synergy H1; BioTek, U.S.A.).

Real-time PCR assay. Approximately 2 μ g of total RNA were reverse transcribed to cDNA by using a cDNA synthesis kit (DRR047A; Takara, Dalian, China) at 37°C for



15 minutes and then at 85°C for 5 seconds. Then, real-time PCR was carried out on a PCR amplification system (Applied Biosystems 7500; Applied Biosystems CO., U.S.A.) using a kit (Fast Start Universal SYBR Green Master, Roche, Swit) and specific primers for HIF-1 α and VEGF. The GAPDH gene was used as an internal reference. The gene expressions of HIF-1 α and VEGF were quantified using 2^{- $\Delta\Delta C_t$} . We obtained data for three independent experiments. The rabbit genes and primer pairs used are listed in Table 2.

Preparation of protein. The harvested retinas were homogenized in lysis buffer (RIPA Lysis Buffer, Cell Signaling Technology, Danvers, U.S.A.). The homogenates were completely lysed on ice for one hour and then centrifuged at 15,000 rpm at 4°C for 20 minutes. The supernatants were collected and their concentrations were detected via a bicinchoninic acid (BCA) protein assay kit (23212; Pierce, U.S.A.). A fraction of the proteins was mixed with 5 \times SDS loading buffer (P0015; Beyotime, Beijing, China), boiled for 5 minutes and then stored at -80°C for Western blotting. The residuals were directly stored at -80°C for enzyme-linked immune sorbent assay (ELISA).

Western blot assay. We processed the Western blotting of retinas for the HIF-1 α protein expression analysis. Fifty μ g of protein per well was loaded on 8% SDS-polyacrylamide electrophoresis gel (SDS-PAGE) (P0012A, Beyotime, Beijing, China), followed by electro-transfer to Polyvinylidene difluoride (PVDF) membranes (Millipore, Billerica, MA, U.S.A) for 2 hours at 200 mA. The membranes were blocked with 5% bovine serum albumin (BSA) (A3808, MultiSciences Biotech Co., Hangzhou, China) in tris-buffered saline with tween (TBST) for 2 hours and incubated with mouse monoclonal anti-HIF-1 α antibody (1 : 1,500; Abcam, New Territories, Hong Kong) at 4°C overnight. After being washed with TBST, the membranes were incubated with a horseradish-peroxidase-(HRP)-linked anti-mouse IgG secondary antibody (1 : 6,000; Cell Signaling Technology, MA, U.S.A.) for 1 hour at room temperature and washed with TBST. β -actin (1 : 5,000; Cell Signaling Technology, MA, U.S.A.) was used as an internal control. The bands were detected by using a chemiluminescence kit (Millipore, Billerica, MA, U.S.A) and the bands' intensities were quantitatively analyzed using Image J 1.43 U software (Wayne Rasband, National Institute of Health, U.S.A.).

Enzyme-linked immune sorbent assay (ELISA). The total protein concentrations of all retinal protein samples were detected prior to the ELISA assay. A VEGF sandwich enzyme-linked immune sorbent assay (ELISA) kit (Human VEGF Immunoassay, DVE00, R&D Systems, U.S.A.) was used to detect the VEGF protein level in the retina. The optical density of each well was measured via a microplate reader (Synergy H1, BioTek, U.S.A.) that subtracted the readings at 540 nm (corrected wavelength) from the readings at 450 nm (detection wavelength). The detection range of the ELISA kit is 20–2,500 pg/ml. The VEGF concentration was estimated from the standard curve. The ELISA procedure was performed according to the manufacturer's instructions and each experiment was repeated three times.

Histopathological and immunohistochemical analysis. Four rabbits from each group were executed at days 90 and 180 postoperatively, and both eyeballs were enucleated for histopathological and immunohistochemical analysis. The eyeballs were fixed in 4% paraformaldehyde for 48 hours and then embedded in paraffin. Sections were cut on a microtome (RM2235; Leica, Germany) at 5 μ m and stained with hematoxylin and eosin (H&E) (C0105; HE kit, Beyotime, Beijing, China).

The retinal sections were heated in a sodium citrate buffer at 95°C for 20 minutes for antigen retrieval. After naturally cooling to room temperature, the sections were blocked in 3% hydrogen peroxide (H₂O₂) for 15 minutes, then blocked in 5% BSA for 30 minutes at 37°C and then incubated with mouse monoclonal anti-HIF-1 α antibody (1 : 200; Abcam, Territories, Hong Kong) and mouse monoclonal anti-VEGF antibody (1 : 200; Abcam, Territories, Hong Kong) at 37°C for 2 hours. After washing with phosphate buffer saline with tween (PBST), the sections were incubated with horseradish-peroxidase-conjugated rabbit anti-mouse IgG antibody (IHC kit, NeoBioscience Technology Co., China) at 37°C for 20 minutes. Then, the sections were stained with diaminobenzidine (IHC kit, NeoBioscience Technology Co., China) for two minutes while being monitored under the microscope (Olympus BX53; Tokyo, Japan), followed by counterstaining with hematoxylin for one minute and mounting with neutral balsam (No.10160; Zhanyun Chemical Co. Ltd., Shanghai, China).

Statistical analysis. All the data were analyzed by using SPSS Statistical Software, version 13.0 (SPSS, Cary, NC, U.S.A.). Data was expressed as mean \pm standard deviation (SD). Statistical differences between treated and contralateral eyes were tested using a paired t-test, and an independent sample t-test was used to test the statistical significances between the treated groups. A value of P less than 0.05 was considered statistically significant.

- Kleinberg, T. T., Tzekov, R. T., Stein, L., Ravi, N. & Kaushal, S. Vitreous substitutes: a comprehensive review. *Surv Ophthalmol.* **56**, 300–323 (2011).
- Sebag, J. & Balazs, E. A. Morphology and ultrastructure of human vitreous fibers. *Invest Ophthalmol Vis Sci.* **30**, 1867–1871 (1989).
- Yurchenko, P. *et al.* Assembly of laminin and type IV collagen into basement membrane networks in extracellular matrix assembly and structure. *San Diego Academic Press*. pp351–388 (1994).
- Reddy, V. N. Dynamics of transport systems in the eye. Friedenwald Lecture. *Invest Ophthalmol Vis Sci.* **18**, 1000–1018 (1979).
- Walker, F. & Patrick, R. S. Constituent monosaccharides and hexosamine concentration of normal human vitreous humour. *Exp Eye Res.* **6**, 227–232 (1967).
- Einar, S. Physiology of vitreous surgery. *Graefes Arch Clin Exp Ophthalmol.* **247**, 147–163 (2009).
- Giordano, G. G. & Refojo, M. F. Silicone oils as vitreous substitutes. *Prog Polymer Sci.* **23**, 509–532 (1998).
- Foster, W. J. Vitreous substitutes. *Expert Rev Ophthalmol.* **3**, 211–218 (2008).
- Lee, B., Litt, M. & Buchsbaum, G. Rheology of the vitreous body. Part I: Viscoelasticity of human vitreous. *Biorheology.* **29**, 521–533 (1992).
- Soman, N. & Banerjee, R. Artificial vitreous replacements. *Biomed Mater Eng.* **13**, 59–74 (2003).
- Azen, S. P. *et al.* Silicone oil in the repair of complex retinal detachments. A prospective observational multicenter study. *Ophthalmology.* **105**, 1587–1597 (1998).
- Zafar, S. *et al.* Outcomes of silicone oil removal. *J Coll Physicians Surg Pak.* **23**, 476–479 (2013).
- Khoroshilova-Maslova, I. P., Nabieva, M. K. & Leparskaia, N. L. Morphogenesis of complications after long-term intraocular silicon oil filling (clinical histopathological study). *Vestn Oftalmol.* **128**, 57–61 (2012).
- Gao, Q. *et al.* A new strategy to replace the natural vitreous by a novel capsular artificial vitreous body with pressure-control valve. *Eye (Lond).* **22**, 461–468 (2008).
- Lin, X. *et al.* Preliminary efficacy and safety of a silicone oil-filled foldable capsular vitreous body in the treatment of severe retinal detachment. *Retina.* **32**, 729–741 (2012).
- Chen, J. *et al.* Clinical device-related article evaluation of morphology and functions of a foldable capsular vitreous body in the rabbit eye. *J Biomed Mater Res B Appl Biomater.* **97**, 396–404 (2011).
- Liu, Y. *et al.* Technical standards of a foldable capsular vitreous body in terms of Mechanical, optical, and biocompatible properties. *Artif Organs.* **34**, 836–845 (2010).
- Wang, P. *et al.* Biocompatibility and retinal support of a foldable capsular vitreous body injected with saline or silicone oil implanted in rabbit eyes. *Clin Experiment Ophthalmol.* **40**, 67–75 (2012).
- Lin, X. *et al.* Evaluation of the flexibility, efficacy, and safety of a foldable capsular vitreous body in the treatment of severe retinal detachment. *Invest Ophthalmol Vis Sci.* **52**, 374–81 (2011).
- Schwartz, S. G., Flynn, H. W. & Mieler, W. F. Update on retinal detachment surgery. *Curr Opin Ophthalmol.* **24**, 255–261 (2013).
- Hayreh, S. S., Rojas, P., Podhajsky, P., Montague, P. & Woolson, R. F. Ocular neovascularization with retinal vascular occlusion-III. Incidence of ocular neovascularization with retinal vein occlusion. *Ophthalmology.* **90**, 488–506 (1983).
- Xiao, D. *et al.* Influence of Dll4 via HIF-1 α -VEGF signaling on the angiogenesis of choroidal neovascularization under hypoxic conditions. *PLoS One.* **6**, e18481 (2011).
- Saint, G. M., Maldonado, A. E. & Amore, P. A. VEGF expression and receptor activation in the choroid during development and in the adult. *Invest Ophthalmol Vis Sci.* **47**, 3135–3142 (2006).
- Zhang, P. *et al.* Rac1 activates HIF-1 in retinal pigment epithelium cells under hypoxia. *Graefes Arch Clin Exp Ophthalmol.* **247**, 633–639 (2009).
- Zhang, P., Wang, Y., Hui, Y., Hu, D. & Wang, H. Inhibition of VEGF expression by targeting HIF-1 alpha with small interference RNA in human RPE cells. *Ophthalmologica.* **221**, 411–417 (2007).
- Feng, S. *et al.* A novel vitreous substitute of using a foldable capsular vitreous body injected with polyvinylalcohol hydrogel. *Sci Rep.* **3**, 1838; doi:10.1038/srep01838 (2013).
- Quaranta, L., Katsanos, A., Russo, A. & Riva, I. 24-hour intraocular pressure and ocular perfusion pressure in glaucoma. *Surv Ophthalmol.* **58**, 26–41 (2013).
- Gray, R. H., Cringle, S. J. & Constable, I. J. Fluorescein angiographic findings in three patients with long-term intravitreal liquid silicone. *Br J Ophthalmol.* **73**, 991–995 (1989).
- Bambas, B., Eckardt, C., Vowinkel, E. & Kruse, H. Toxic substances with silicone oil after intraocular injections. *Ophthalmologie.* **92**, 663–667 (1995).
- Mukai, N., Lee, P. & Schepens, C. L. Intravitreal injection of silicone: an experimental study. 2: Histochemistry and electron microscopy. *Ann Ophthalmol.* **4**, 273–287 (1972).
- Linden, T. *et al.* The antimycotic ciclopirox olamine induces HIF-1 α stability, VEGF expression and angiogenesis. *FASEB J.* **17**, 761–763 (2003).
- O'Donnell, J. L. *et al.* Oncological implications of hypoxia inducible factor-1 α (HIF-1 α) expression. *Cancer Treat Rev.* **32**, 407–416 (2006).
- Wang, G. L., Jiang, B. H., Rue, E. A. & Semenza, G. L. Hypoxia inducible factor 1 is a basic loop helix loop PAS heterodimer regulated by cellular O₂ tension. *Proc Natl Acad Sci USA.* **92**, 5510–5514 (1995).
- Weidemann, A. *et al.* Astrocyte hypoxic response is essential for pathological but not developmental angiogenesis of the retina. *Glia.* **58**, 1177–1185 (2010).
- Carmeliet, P. *et al.* Abnormal blood vessel development and lethality in embryos lacking a single VEGF allele. *Nature.* **380**, 435–439 (1996).



36. Ferrara, N. *et al.* Heterozygous embryonic lethality induced by targeted inactivation of the VEGF gene. *Nature*. **380**, 439–442 (1996).
37. Kim, I. *et al.* Constitutive expression of VEGF, VEGFR-1, and VEGFR-2 in normal eyes. *Invest Ophthalmol Vis Sci*. **40**, 2115–2121 (1999).
38. Adamis, A. P. *et al.* Inhibition of vascular endothelial growth factor prevents retinal ischemia-associated iris neovascularization in a nonhuman primate. *Arch Ophthalmol*. **114**, 66–71 (1996).
39. Aiello, L. P. *et al.* Suppression of retinal neo-vascularization in vivo by inhibition of vascular endothelial growth factor (VEGF) using soluble VEGF-receptor chimeric proteins. *Proc Natl Acad Sci USA*. **92**, 10457–10461 (1995).
40. Linden, T. *et al.* The antimycotic ciclopirox olamine induces HIF-1 α stability, VEGF expression and angiogenesis. *FASEB J*. **17**, 761–763 (2003).
41. Liu, Y., Cox, S. R., Morita, T. & Kourembanas, S. Hypoxia regulates vascular endothelial growth factor gene expression in endothelial cells. *Circ Res*. **77**, 638–643 (1995).
42. Shen, M., Gao, J., Li, J. & Su, J. Effect of stimulation frequency on angiogenesis and gene expression in ischemic skeletal muscle of rabbit. *Can J Physiol Pharmacol*. **87**, 396–401 (2009).
43. Ozaki, H. *et al.* Hypoxia inducible factor-1 α is increased in ischemic retina: temporal and spatial correlation with VEGF expression. *Invest Ophthalmol Vis Sci*. **40**, 182–189 (1999).
44. Shima, D. T., Deutsch, U. & D'Amore, P. A. Hypoxic induction of vascular endothelial growth factor (VEGF) in human epithelial cells is mediated by increases in mRNA stability. *FEBS Lett*. **370**, 203–208 (1995).
45. Levy, A. P., Levy, N. S. & Goldberg, M. A. Post-transcriptional regulation of vascular endothelial growth factor by hypoxia. *Biol Chem*. **271**, 2746–2753 (1996).
46. Shui, Y. B. *et al.* Oxygen distribution in the rabbit eye and oxygen consumption by the lens. *Invest Ophthalmol Vis Sci*. **47**, 1571–1580 (2006).
47. Chirila, T. V., Tahija, S., Hong, Y., Vijayasekaran, S. & Constable, I. J. Synthetic polymers as materials for artificial vitreous body: review and recent advances. *J Biomater Appl*. **9**, 121–137 (1994).
48. Bairo, F. Towards an ideal biomaterial for vitreous replacement: Historical overview and future trends. *Acta Biomater*. **7**, 921–935 (2011).
49. Grogan, A. T. & Pinczewski, W. V. The role of molecular diffusion processes in tertiary CO₂ flooding. *J Petrol Technol*. **39**, 591–602 (1987).
50. Othmef, D. F. & Thakar, M. S. Correlating diffusion of coefficient in liquids. *Ind Eng Chem*. **45**, 589–593 (1953).
51. De Juan, E. Jr., Hardy, M., Hatchell, D. L. & Hatchell, M. C. Oxygen distribution in the rabbits eye and oxygen consumption by the lens. *Arch Ophthalmol*. **104**, 1063–1064 (1986).
52. Aim, A. & Bill, A. The oxygen supply to the retina: I. Effects of changes in intraocular and arterial blood pressures and in arterial PO₂ and PCO₂ on the oxygen tension in the vitreous body of the cat. *Acta Physiol Scand*. **84**, 261–274 (1972).
53. Denis, P., Ricky, L., Liana, C. & Ronald, J. Neufeld, J. Microencapsulation of silicone oils within polyamide-polyethylenimine membranes as oxygen carriers for bioreactor oxygenation. *J. Clin. Tech. Biotechnol*. **57**, 253–263 (1993).
54. Barbazetto, I. A. *et al.* Oxygen tension in the rabbit lens and vitreous before and after vitrectomy. *Exp Eye Res*. **78**, 917–924 (2004).
55. Xiao, Q. C. *et al.* Protein kinase C α downregulation via siRNA-PKC α released from foldable capsular vitreous body in cultured human retinal pigment epithelium cells. *Int J Nanomedicine*. **6**, 1303–1311 (2011).
56. Jiang, Z. *et al.* Evaluation of the levofloxacin release characters from a rabbit foldable capsular vitreous body. *Int J Nanomedicine*. **7**, 1–10 (2012).
57. Zheng, H. *et al.* Evaluation of 5-fluorouracil released from a foldable capsular vitreous body in vitro and in vivo. *Graefes Arch Clin Exp Ophthalmol*. **250**, 751–759 (2012).
58. Kampik, A. & Gandorfer, A. Silicone oil removal strategies. *Semin Ophthalmol*. **15**, 88–91 (2000).
59. Pereira, F. Q., Bercht, B. S., Soares, M. G., da Mota, M. G. & Pigatto, J. A. Comparison of a rebound and an applanation tonometer for measuring intraocular pressure in normal rabbits. *Vet Ophthalmol*. **14**, 321–326 (2011).

Acknowledgments

This study was supported by the Youth Fund of the State Key Laboratory of Ophthalmology (2011Q10) and the National Science & Technology Pillar Program of the Twelfth Five-year Plan (2012BAI08B02).

Author contributions

W.Y., Y.Q.L. and Q.Y.G. conceived and designed the study and wrote the paper; W.Y., Y.G.Y., Y.Z., Z.H. and S.Y.M. conducted the animal experiments. W.Y. and X.B.Q. performed the molecular biological and histopathologic experiments in vitro. Y.J.L. fabricated the FCVBs.

Additional information

Competing financial interests: The authors declare no competing financial interests.

How to cite this article: Yang, W. *et al.* Preliminary Study on Retinal Vascular and Oxygen-related Changes after Long-term Silicone Oil and Foldable Capsular Vitreous Body Tamponade. *Sci. Rep.* **4**, 5272; DOI:10.1038/srep05272 (2014).



This work is licensed under a Creative Commons Attribution-NonCommercial-NoDerivs 4.0 International License. The images or other third party material in this article are included in the article's Creative Commons license, unless indicated otherwise in the credit line; if the material is not included under the Creative Commons license, users will need to obtain permission from the license holder in order to reproduce the material. To view a copy of this license, visit <http://creativecommons.org/licenses/by-nc-nd/4.0/>